

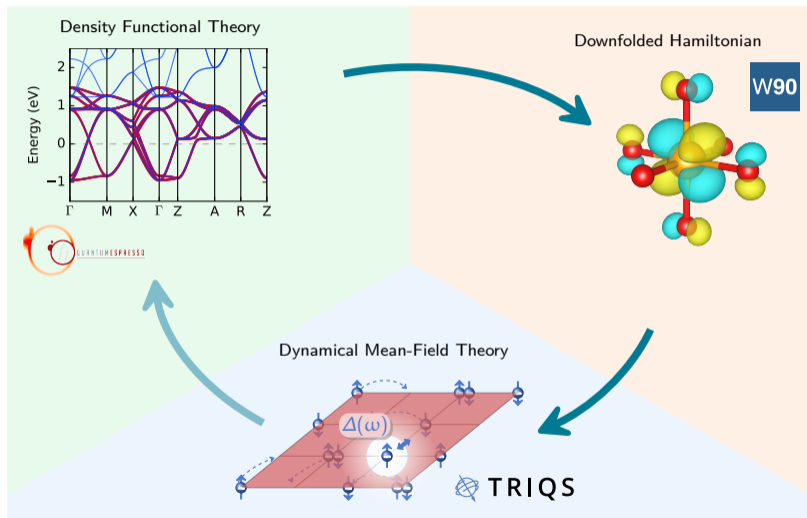
TRIQS Summer School 2023

Ab initio description of strongly correlated materials: combining density functional theory plus and dynamical mean-field theory

Sophie Beck
31st August 2023



Density Functional Theory + Dynamical Mean-Field Theory

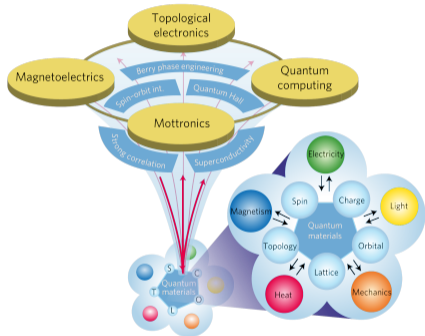


1. Introduction

2. DFT+DMFT

- DMFT recap
- Ab initio electronic structure
- DFT+DMFT ingredients
- Impurity solvers
- Charge self-consistency
- Post-processing

3. Summary

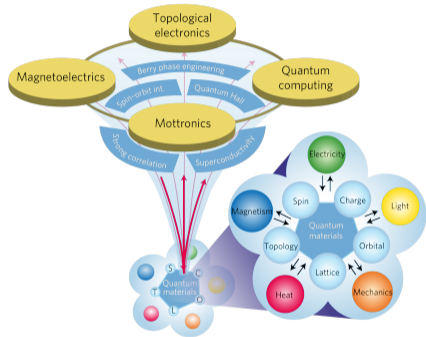


REVIEW ARTICLES

NATURE PHYSICS DOI: 10.1038/NPHYS4274

Table 1 | Summary of various emergent functions discussed in this article.

Emergent functions	Key concept	Control parameter	Bottleneck/key experiment	Target industry
Mottronics	Electron correlation	Band-filling Bandwidth	E-field switching at RT Above-RT superconductor	Low-energy-cost electronics Energy harvesting/saving
Magnetoelectrics	Spin-orbit interaction	Broken symmetries both in space and time	E-field switching at RT Ultrafast photo-switching	Low-energy-cost electronics Information technology
Topological electronics	Berry phase	Band structure design Spin texture	Zero-field edge current at RT Skyrmionic circuit	Information technology Energy harvesting
Quantum computing	Quantum coherence	Nanomaterials design Topological protection	Qubit/photon interface Quantum simulator	Quantum computer Information security

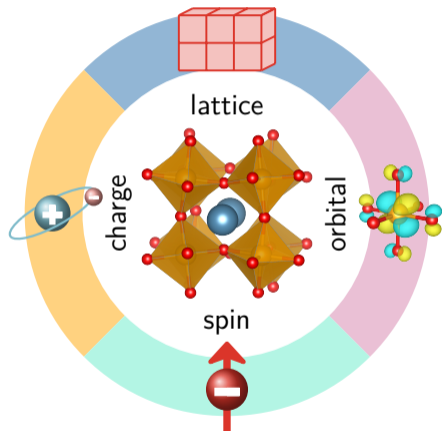


REVIEW ARTICLES

NATURE PHYSICS DOI: 10.1038/NPHYS4274

Table 1 | Summary of various emergent functions discussed in this article.

Emergent functions	Key concept	Control parameter	Bottleneck/key experiment	Target industry
Mottronics	Electron correlation	Band-filling Bandwidth	E-field switching at RT Above-RT superconductor	Low-energy-cost electronics Energy harvesting/saving
Magnetoelectrics	Spin-orbit interaction	Broken symmetries both in space and time	E-field switching at RT Ultrafast photo-switching	Low-energy-cost electronics Information technology
Topological electronics	Berry phase	Band structure design Spin texture	Zero-field edge current at RT Skyrmionic circuit	Information technology Energy harvesting
Quantum computing	Quantum coherence	Nanomaterials design Topological protection	Qubit/photon interface Quantum simulator	Quantum computer Information security



- sensitive to small changes in external parameters:
 - temperature
 - pressure
 - doping
 - ...
- emerging phenomena:
 - high T_C superconductivity
 - colossal magnetoresistance
 - Mott physics
 - ...

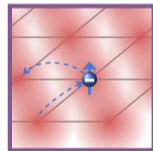
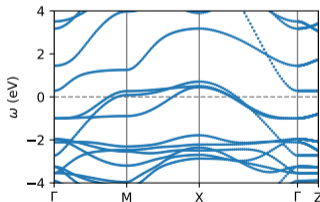
Correlated d -/ f -shells

	1	2	3	4	5	6	7	8	9	10	11	12	13	14	15	16	17	18						
													Pnictogens		Chalcogens		Halogens							
																			Atomic Symbol					
																			Name					
																			Weight					
1	1 H Hydrogen -1.1	2 He Helium																						
2	3 Li Lithium 1	4 Be Beryllium 2																						
3	11 Na Sodium 1	12 Mg Magnesium 2																5 B Boron 3	6 C Carbon -4.4	7 N Nitrogen -3.35	8 O Oxygen -2	9 F Fluorine -1	10 Ne Neon	
4	19 K Potassium 1	20 Ca Calcium 2	21 Sc Scandium 3	22 Ti Titanium 4	23 V Vanadium 5	24 Cr Chromium 3.6	25 Mn Manganese 2.47	26 Fe Iron 2.3	27 Co Cobalt 2.3	28 Ni Nickel 2	29 Cu Copper 2	30 Zn Zinc	31 Ga Gallium	32 Ge Germanium -4.24	33 As Arsenic -3.35	34 Se Selenium -2.246	35 Br Bromine -1.135	36 Kr Krypton 2						
5	37 Rb Rubidium 1	38 Sr Strontium 2	39 Y Yttrium 3	40 Zr Zirconium 4	41 Nb Niobium 5	42 Mo Molybdenum 4.6	43 Tc Technetium 4.7	44 Ru Ruthenium 3.4	45 Rh Rhodium 3	46 Pd Palladium 2.4	47 Ag Silver 1	48 Cd Cadmium 2	49 In Indium	50 Sn Tin -4.24	51 Sb Antimony -3.35	52 Te Tellurium -2.246	53 I Iodine -1.1357	54 Xe Xenon 2.46						
6	55 Cs Caesium 1	56 Ba Barium 2	57-71	72 Hf Hafnium 4	73 Ta Tantalum 5	74 W Tungsten 4.6	75 Re Rhenium 4	76 Os Osmium 4	77 Ir Iridium 3.4	78 Pt Platinum 2.4	79 Au Gold 3	80 Hg Mercury 1.2	81 Tl Thallium 2.4	82 Pb Lead 2.4	83 Bi Bismuth 3	84 Po Polonium -2.24	85 At Astatine -1.1	86 Rn Radon 2						
7	87 Fr Francium 1	88 Ra Radium 2	89-103	104 Rf Rutherfordium 4	105 Db Dubnium 5	106 Sg Seaborgium 6	107 Bh Bohrium 7	108 Hs Hassium 8	109 Mt Meitnerium	110 Ds Darmstadtium	111 Rg Roentgenium	112 Cn Copernicium	113 Nh Nihonium	114 Fl Flerovium	115 Mc Moscovium	116 Lv Livermorium	117 Ts Tennessine	118 Og Oganesson						
Oxidation states are the number of electrons added to or removed from an element when it forms a chemical compound.																								
6	57 La Lanthanum 3	58 Ce Cerium 3.4	59 Pr Praseodymium 3	60 Nd Neodymium 3	61 Pm Promethium 3	62 Sm Samarium 3	63 Eu Europium 2.3	64 Gd Gadolinium 3	65 Tb Terbium 3	66 Dy Dysprosium 3	67 Ho Holmium 3	68 Er Erbium 3	69 Tm Thulium 3	70 Yb Ytterbium 3	71 Lu Lutetium 3									
7	89 Ac Actinium 3	90 Th Thorium 4	91 Pa Protactinium 5	92 U Uranium 6	93 Np Neptunium 5	94 Pu Plutonium 4	95 Am Americium 3	96 Cm Curium 3	97 Bk Berkelium 3	98 Cf Californium 3	99 Es Einsteinium 3	100 Fm Fermium 3	101 Md Mendelevium 3	102 No Nobelium 2	103 Lr Lawrencium 3									

effective single-particle picture

- weakly correlated systems
- density functional theory
- Fermi liquid theory

$$\begin{aligned}\Psi(\mathbf{x}_1, \mathbf{x}_2) &= \frac{1}{\sqrt{2}} \{ \chi_1(\mathbf{x}_1) \chi_2(\mathbf{x}_2) - \chi_1(\mathbf{x}_2) \chi_2(\mathbf{x}_1) \} \\ &= \frac{1}{\sqrt{2}} \begin{vmatrix} \chi_1(\mathbf{x}_1) & \chi_2(\mathbf{x}_1) \\ \chi_1(\mathbf{x}_2) & \chi_2(\mathbf{x}_2) \end{vmatrix},\end{aligned}$$



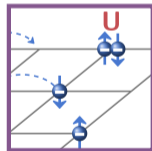
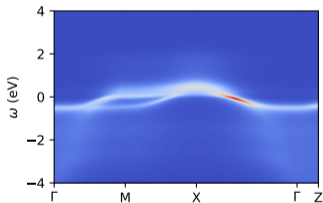
effective single-particle picture

- weakly correlated systems
- density functional theory
- Fermi liquid theory

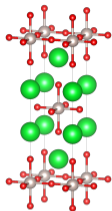
strongly correlated systems

- breakdown of single-particle picture
- strong local Coulomb interaction U
- between ionic localization and itinerant behavior

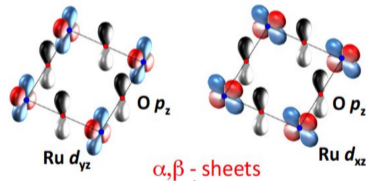
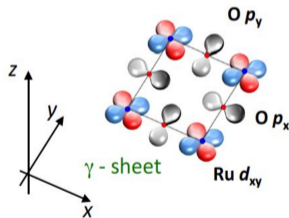
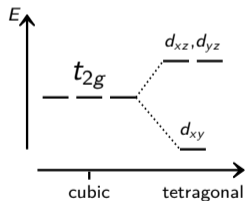
$$\begin{aligned}\Psi(\mathbf{x}_1, \mathbf{x}_2) &= \frac{1}{\sqrt{2}} \{ \chi_1(\mathbf{x}_1) \chi_2(\mathbf{x}_2) - \chi_1(\mathbf{x}_2) \chi_2(\mathbf{x}_1) \} \\ &= \frac{1}{\sqrt{2}} \begin{vmatrix} \chi_1(\mathbf{x}_1) & \chi_2(\mathbf{x}_1) \\ \chi_1(\mathbf{x}_2) & \chi_2(\mathbf{x}_2) \end{vmatrix},\end{aligned}$$



Case study: Fermi surface of Sr_2RuO_4

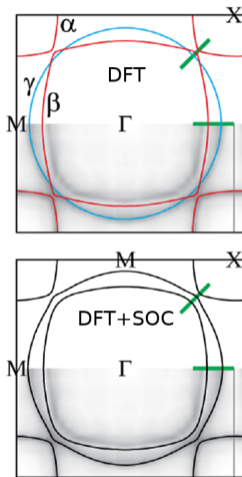


- strong correlations ($U = 2.3$ eV)
- Hund physics ($J = 0.4$ eV)
- spin-orbit coupling ($\lambda = 0.1 - 0.2$ eV)
- Fermi liquid ($T_{\text{FL}} \approx 25$ K)
- superconductivity ($T_{\text{C}} \approx 1.5$ K)
- Van Hove singularity close to E_{F}



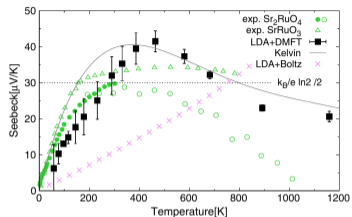
Where DFT may be insufficient

Fermi surface



M. W. Haverkort *et al.*, Phys. Rev. Lett. 101, 026406 (2008)

Seebeck

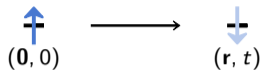


- also: mass enhancement, orbital occupations, optics, SOC, ...
- **more obvious**: local-moment paramagnet (**Mott insulator**) versus (anti-)ferromagnet or non-magnetic metal in DFT

J. Mravlje, A. Georges, Phys. Rev. Lett. 117, 036401 (2016)

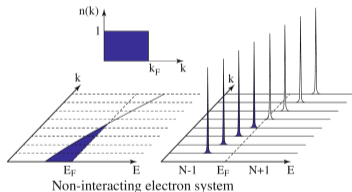
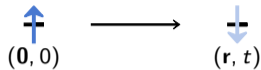
Spectral function $A(\mathbf{k}, \omega)$

$$A(\mathbf{k}, \omega) = \frac{1}{\pi} \text{Im} \int d\mathbf{r} \int dt e^{i(\mathbf{k}\mathbf{r} - \omega t)} \underbrace{i\theta(t) \langle [\Psi(\mathbf{r}, t), \Psi^\dagger(\mathbf{0}, 0)] \rangle}_{G^R(\mathbf{r}, t)}$$



Spectral function $A(\mathbf{k}, \omega)$ - non-interacting

$$A(\mathbf{k}, \omega) = \frac{1}{\pi} \text{Im} \int d\mathbf{r} \int dt e^{i(\mathbf{k}\mathbf{r} - \omega t)} \underbrace{i\theta(t) \langle [\Psi(\mathbf{r}, t), \Psi^\dagger(\mathbf{0}, 0)] \rangle}_{G^R(\mathbf{r}, t)}$$

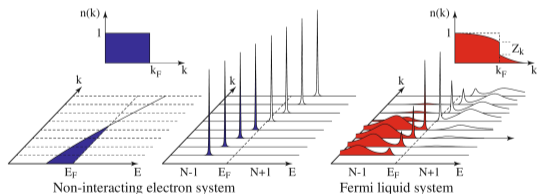
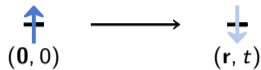


$$G(\mathbf{k}, \omega) = \frac{1}{\omega - \epsilon_{\mathbf{k}} + i\eta}$$

$$A(\mathbf{k}, \omega) = -\frac{1}{\pi} \delta(\omega - \epsilon_{\mathbf{k}})$$

Spectral function $A(\mathbf{k}, \omega)$ - interacting

$$A(\mathbf{k}, \omega) = \frac{1}{\pi} \text{Im} \int d\mathbf{r} \int dt e^{i(\mathbf{k}\mathbf{r} - \omega t)} \underbrace{i\theta(t) \langle [\Psi(\mathbf{r}, t), \Psi^\dagger(\mathbf{0}, 0)] \rangle}_{G^R(\mathbf{r}, t)}$$



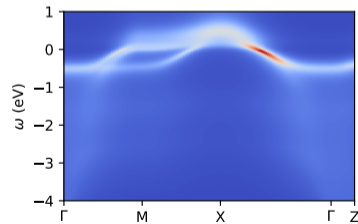
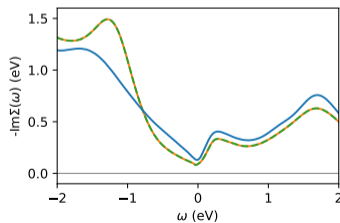
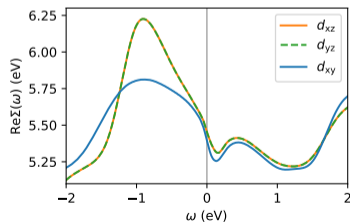
$$G(\mathbf{k}, \omega) = \frac{1}{\omega - \epsilon_{\mathbf{k}} - \Sigma(\omega)}$$

$$\Sigma(\omega) = \Sigma'(\omega) + i\Sigma''(\omega)$$

$$A(\mathbf{k}, \omega) = -\frac{1}{\pi} \frac{\Sigma''(\omega)}{(\omega - \epsilon_{\mathbf{k}} - \Sigma'(\omega))^2 + \Sigma''(\omega)^2}$$

$$G(\mathbf{k}, \omega) = \frac{1}{\omega - \epsilon_{\mathbf{k}} - \Sigma(\omega)}$$

$$\text{with } \Sigma(\omega) = \Sigma'(\omega) + i\Sigma''(\omega)$$



$$G(\mathbf{k}, \omega) = \frac{Z(\epsilon_{\mathbf{k}}^*)}{\omega - \epsilon_{\mathbf{k}}^* - i\Gamma(\epsilon_{\mathbf{k}}^*)} + G_{\text{incoh}}$$

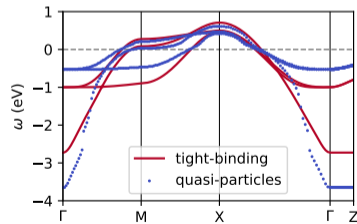
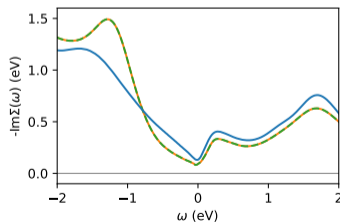
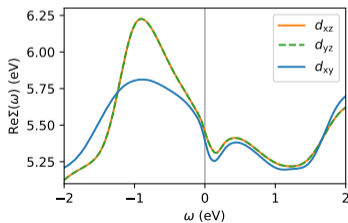
if $\Sigma''(\omega)$ not too large: quasiparticles

- $\epsilon_{\mathbf{k}}^*$ quasiparticle dispersion
- Z quasiparticle renormalization
- Γ scattering rate/inverse lifetime

$$\epsilon_{\mathbf{k}}^* = \epsilon_{\mathbf{k}} + \Sigma'(\epsilon_{\mathbf{k}}^*)$$

$$Z(\omega) = \left[1 - \frac{\partial \Sigma'(\omega)}{\partial \omega}\right]^{-1}$$

$$\Gamma(\omega) = -Z(\omega)\Sigma''(\omega)$$



$$G(\mathbf{k}, \omega) = \frac{Z}{\omega - \epsilon_{\mathbf{k}}^* - i\Gamma} + G_{\text{incoh}}$$

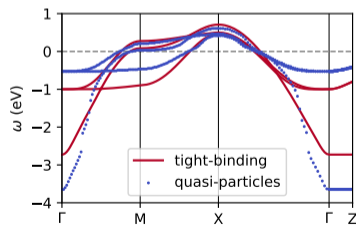
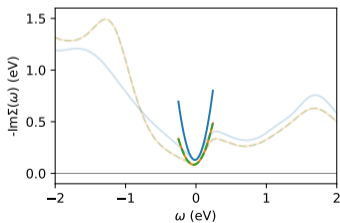
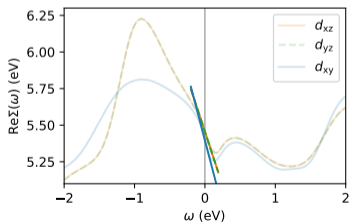
if $\Sigma''(\omega)$ not too large and near $\omega = 0$

- $\epsilon_{\mathbf{k}}^*$ quasiparticle dispersion
- Z quasiparticle renormalization
- Γ scattering rate/inverse lifetime

$$\epsilon_{\mathbf{k}}^* = Z(\epsilon_{\mathbf{k}} + \Sigma'(0))$$

$$Z = \left[1 - \frac{\partial \Sigma'(\omega)}{\partial \omega} \Big|_{\omega=0}\right]^{-1} = \frac{m}{m^*}$$

$$\Gamma = -Z\Sigma''(0)$$



$$G(\mathbf{k}, \omega) = \frac{Z}{\omega - \epsilon_{\mathbf{k}}^* - i\Gamma} + G_{\text{incoh}}$$

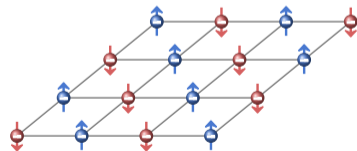
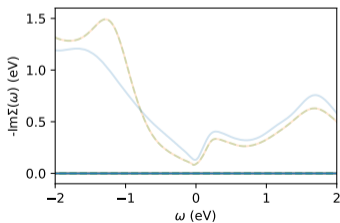
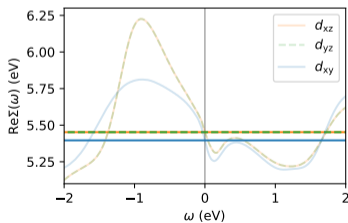
if $\Sigma''(\omega)$ not too large and near $\omega = 0$

- $\epsilon_{\mathbf{k}}^*$ quasiparticle dispersion
- Z quasiparticle renormalization
- Γ scattering rate/inverse lifetime

$$\epsilon_{\mathbf{k}}^* = \epsilon_{\mathbf{k}} + \Sigma'(0)$$

$$Z = \left[1 - \frac{\partial \Sigma'(0)}{\partial \omega}\right]^{-1} = 1$$

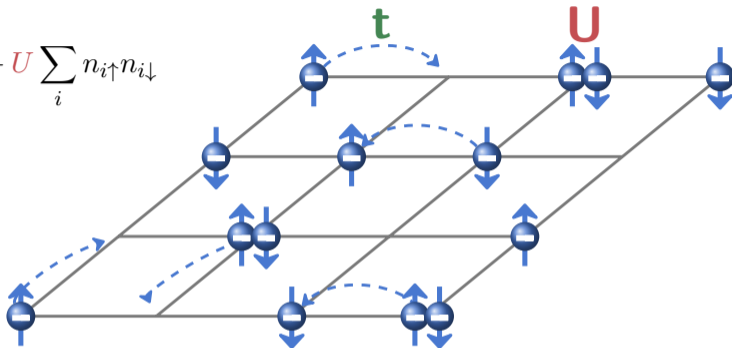
$$\Gamma \rightarrow 0$$



- **situation:** complex physics arising from strong local Coulomb interaction in partially filled orbitals in strongly correlated materials
- **goal:** ab-initio, material-realistic description
- **challenge:** combining localized, atomic-like and itinerant electronic behavior
- **ansatz:** DFT+DMFT, downfolding & embedding
- **ingredients:** hoppings t and Coulomb repulsion U for downfolded model, projector functions P to transform from/to full system
- **example:** Fermi surface of Sr_2RuO_4

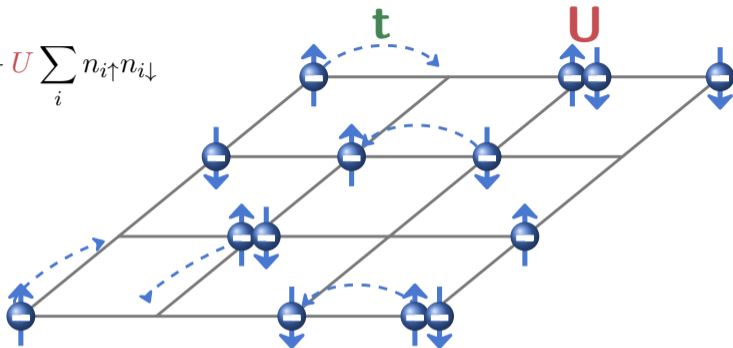
recap: the Hubbard model

$$H = - \sum_{ij,\sigma} t_{ij} c_{i\sigma}^\dagger c_{j\sigma} + U \sum_i n_{i\uparrow} n_{i\downarrow}$$

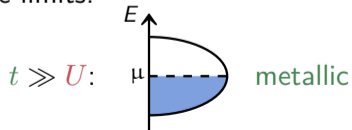


recap: the Hubbard model

$$H = - \sum_{ij,\sigma} t_{ij} c_{i\sigma}^\dagger c_{j\sigma} + U \sum_i n_{i\uparrow} n_{i\downarrow}$$

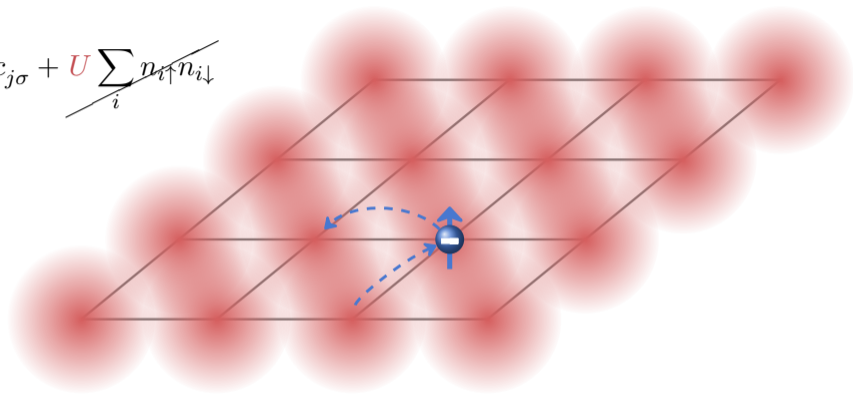


In the limits:

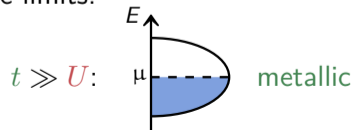


recap: the Hubbard model

$$H = - \sum_{ij,\sigma} t_{ij} c_{i\sigma}^\dagger c_{j\sigma} + U \sum_i n_{i\uparrow} n_{i\downarrow}$$

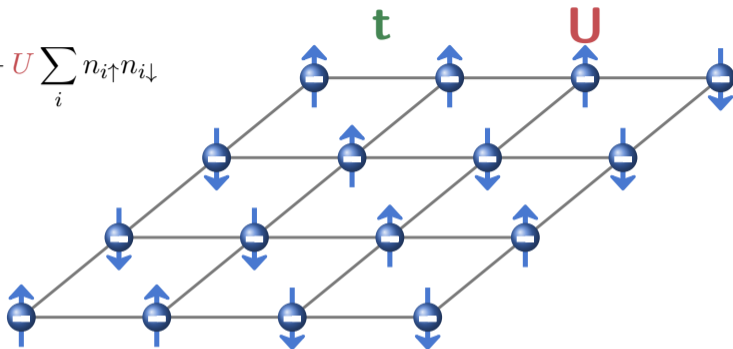


In the limits:

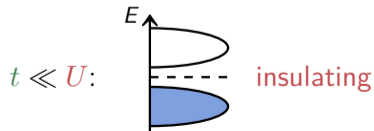
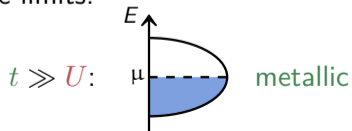


recap: the Hubbard model

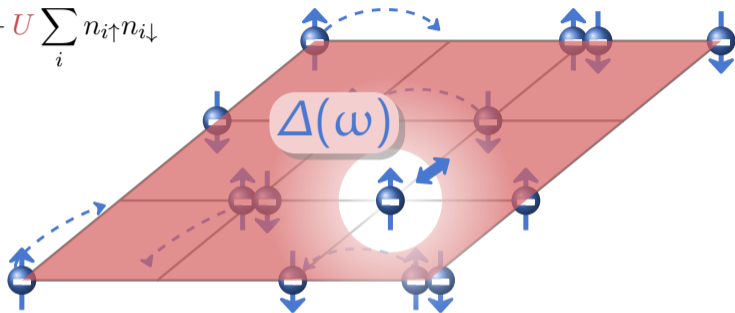
$$H = - \sum_{ij,\sigma} t_{ij} c_{i\sigma}^\dagger c_{j\sigma} + U \sum_i n_{i\uparrow} n_{i\downarrow}$$



In the limits:



$$H = - \sum_{ij,\sigma} t_{ij} c_{i\sigma}^\dagger c_{j\sigma} + U \sum_i n_{i\uparrow} n_{i\downarrow}$$



- map lattice to effective impurity model (AIM) embedded in bath
- impurity-bath coupling $\Delta(\omega)$ determined self-consistently
- basic ingredients: t, U

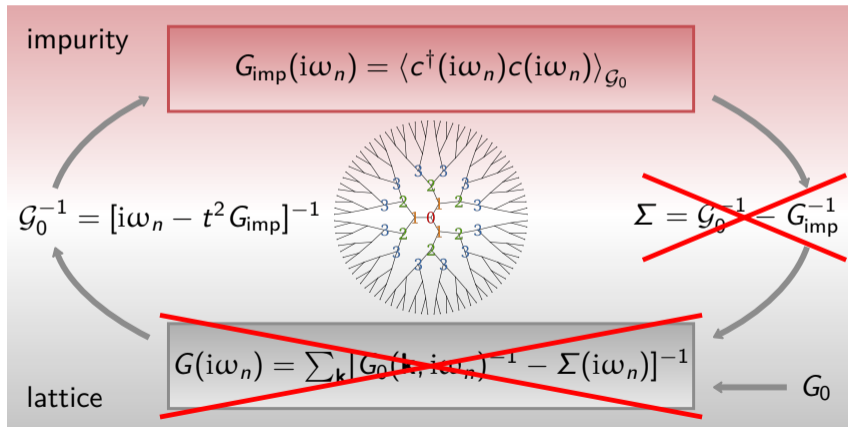
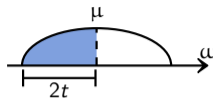
W. Metzner and D. Vollhardt, Phys. Rev. Lett. 62, 3 (1989)

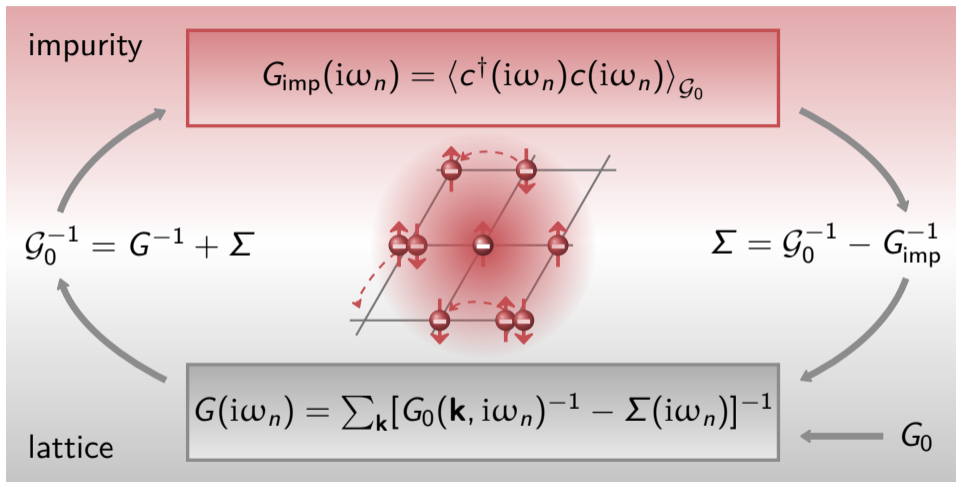
A. Georges and G. Kotliar, Phys. Rev. B 45, 12 (1992)

DMFT self-consistency - example: Bethe lattice

$z \rightarrow \infty$:

$$\rho(\omega) = \frac{1}{2\pi t^2} \sqrt{4t^2 - \omega^2}$$



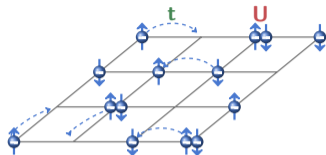


- basic ingredients: t , U , and P

From many-body to effective one-body problem

electronic Schrödinger equation:

$$\hat{H}\Psi(\mathbf{r}_1, \dots, \mathbf{r}_N) = \epsilon\Psi(\mathbf{r}_1, \dots, \mathbf{r}_N)$$



with

$$\hat{H} = -\sum_i \frac{\hbar^2 \nabla_i^2}{2m} + \sum_{i<j} \frac{e^2}{|\mathbf{r}_i - \mathbf{r}_j|} + \sum_i^N v_{\text{ext}}(\mathbf{r}_i) = T + U + V_{\text{ext}}$$

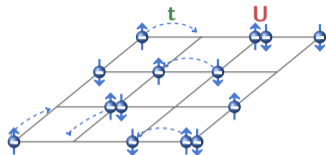
in second quantization:

$$\hat{H} = \sum_{ij} t_{ij} c_i^\dagger c_j + \sum_{ijkl} U_{ijkl} c_i^\dagger c_j^\dagger c_l c_k$$

From many-body to effective one-body problem

electronic Schrödinger equation:

$$\hat{H}\Psi(\mathbf{r}_1, \dots, \mathbf{r}_N) = \epsilon\Psi(\mathbf{r}_1, \dots, \mathbf{r}_N)$$



with

$$\hat{H} = -\sum_i \frac{\hbar^2 \nabla_i^2}{2m} + \sum_{i<j} \frac{e^2}{|\mathbf{r}_i - \mathbf{r}_j|} + \sum_i^N v_{\text{ext}}(\mathbf{r}_i) = T + U + V_{\text{ext}}$$

in second quantization:

$$\hat{H} = \sum_{ij} t_{ij} c_i^\dagger c_j + \sum_{ijkl} U_{ijkl} c_i^\dagger c_j^\dagger c_l c_k \rightarrow \hat{H}_{\text{DFT}} = \sum_{ij} \tilde{t}_{ij} c_i^\dagger c_j$$

1. Hohenberg-Kohn theorem: the external potential (and total energy) is a unique functional of the electron density: $\Psi(\mathbf{r}_1, \dots, \mathbf{r}_N) \rightarrow \rho(\mathbf{r})$

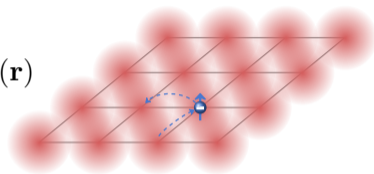
$$\rho(\mathbf{r}) = N \int d^3\mathbf{r}_2 \cdots \int d^3\mathbf{r}_N |\Psi(\mathbf{r}, \mathbf{r}_2, \cdots, \mathbf{r}_N)|^2$$

2. Hohenberg-Kohn theorem: the ground-state charge density ρ_0 minimises the energy functional, i.e. yielding the ground-state energy E_0

$$E[\rho_0] \leq E[\rho] = \min_{\Psi \rightarrow \rho_0} \langle \Psi | T + U + V_{\text{ext}} | \Psi \rangle$$

Recast full system into a fictitious, auxiliary system of separable Kohn-Sham orbitals $\{\psi_n\}$, that generates the same density as the original one

$$\left[-\frac{\hbar^2}{2m} \nabla^2 + v_{\text{eff}}(\mathbf{r}) \right] \psi_n(\mathbf{r}) = \epsilon_n \psi_n(\mathbf{r})$$



$$v_{\text{eff}}(\mathbf{r}) = v_{\text{H}}[\rho](\mathbf{r}) + \frac{\delta E_{\text{XC}}[\rho]}{\delta \rho(\mathbf{r})} + v_{\text{ext}}(\mathbf{r})$$

- solution is found self-consistently
- exchange-correlation potential is the only unknown
- Kohn-Sham orbital energies have little physical meaning

$$\rightarrow \hat{H}_{\text{KS}} = \sum_{ij} \tilde{t}_{ij} c_i^\dagger c_j$$

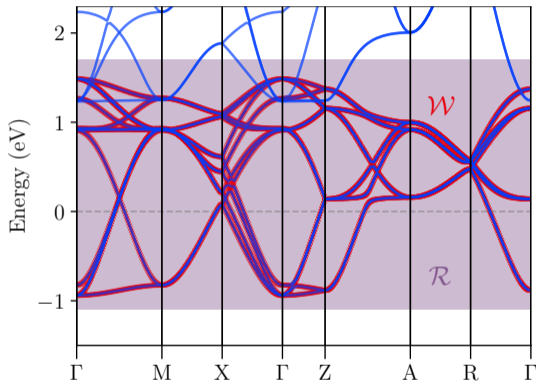
- partitioning of the system
- maximally localized Wannier functions $|\mathbf{R}j\rangle$ from Kohn-Sham states $|\psi_{n\mathbf{k}}\rangle$:

$$|\psi_{j\mathbf{k}}^W\rangle = \sum_n U_{\mathbf{k},nj} |\psi_{n\mathbf{k}}\rangle$$

$$|\mathbf{R}j\rangle = \frac{V}{(2\pi)^3} \int_{\text{BZ}} d\mathbf{k} e^{-i\mathbf{k}\mathbf{R}} |\psi_{j\mathbf{k}}^W\rangle$$

hopping elements:

$$t_{ij}(\mathbf{R}) = \langle 0i | \hat{H}^{\text{KS}} | \mathbf{R}j \rangle$$



DFT+DMFT ingredients: projector functions P

lattice Green's function:

$$\hat{G}(\mathbf{k}, i\omega_n) = \sum_{mn} \left[i\omega_n + \mu - \hat{\epsilon}(\mathbf{k}) - \Delta\hat{\Sigma}(\mathbf{k}, i\omega_n) \right]_{mn}^{-1} |\psi_{m\mathbf{k}}\rangle \langle \psi_{n\mathbf{k}}|$$

downfolding:

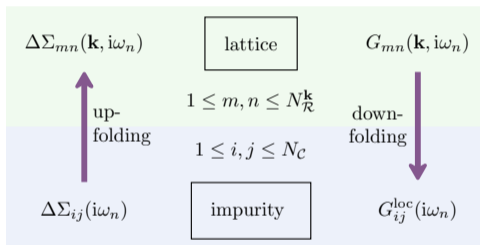
$$G_{ij,\mathcal{R}}^{\text{loc}}(i\omega_n) = \sum_{\mathbf{k}, mn} P_{im}^{\mathcal{R}}(\mathbf{k}) G_{mn}(\mathbf{k}, i\omega_n) P_{nj}^{\mathcal{R}*}(\mathbf{k})$$

with projector onto orbital j at atomic site \mathcal{R} :

$$P_{jn}^{\mathcal{R}}(\mathbf{k}) = \langle \psi_{\mathcal{R}j\mathbf{k}}^{\text{W}} | \psi_{n\mathbf{k}} \rangle$$

upfolding:

$$\Delta\Sigma_{mn}(\mathbf{k}, i\omega_n) = \sum_{\mathcal{R}, ij} P_{mi}^{\mathcal{R}*}(\mathbf{k}) \Delta\Sigma_{ij}^{\mathcal{R}}(i\omega_n) P_{jn}^{\mathcal{R}}(\mathbf{k})$$



- basis transformation
- entanglement
- local symmetries

- E_U is a functional of the orbital occupations, but E_{XC} is a non-linear functional of the total electron density
- ill-posed problem due to the formally incompatible footing: diagrammatic vs. non-perturbative
- different analytic, *phenomenological* expressions have been proposed: FLL, AMF, ANI, Kunes, nominal...
- remedy: $GW+DMFT$

$$\Delta\Sigma_{ij}^{\mathcal{R}}(i\omega_n) = \Sigma_{ij}^{\mathcal{R}}(i\omega_n) - \Sigma_{DC}$$

$$E_{\text{DFT}+U}[\rho] = E_{\text{DFT}}[\rho] + E_U[n_{ij}^{\sigma}] - E_{\text{DC}}$$

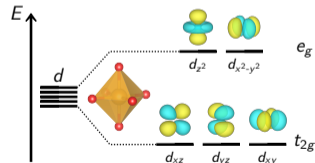
$$E_{\text{XC}} \approx E_{\text{XC}}^{\text{LDA}}[\rho] = \int d\mathbf{r} \epsilon_{\text{XC}}^{\text{hom}}[\rho(\mathbf{r})]\rho(\mathbf{r})$$

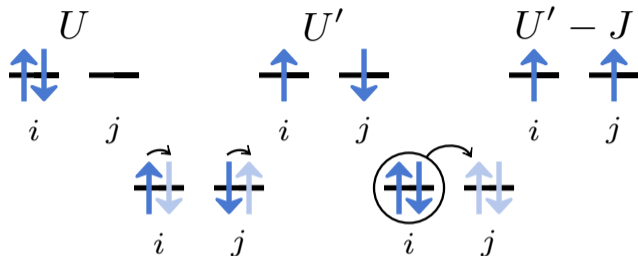
$$E_{\text{XC}}[n_{ij}^{\sigma}]?$$

$$\hat{H}_{\text{int}} = \frac{1}{2} \sum_{ijkl}^{\text{at } \mathcal{R}} U_{ijkl} c_i^\dagger c_j^\dagger c_l c_k$$

$$V_{ijkl} = \int d^3\mathbf{r} d^3\mathbf{r}' w_i^*(\mathbf{r}) w_j^*(\mathbf{r}') \frac{e^2}{|\mathbf{r} - \mathbf{r}'|} w_l(\mathbf{r}') w_k(\mathbf{r})$$

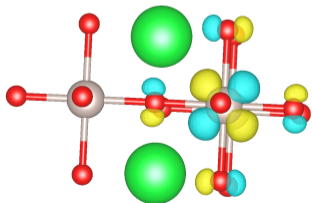
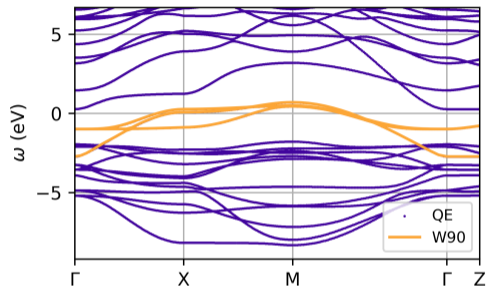
- complicated 4-rank tensor
- use symmetries to reduce complexity
- for cubic systems: Hubbard-Kanamori parametrization
- for spherical systems: Slater parametrization





$$\hat{H}_U = U \sum_i n_{i\uparrow} n_{i\downarrow} + U' \sum_{i \neq j} n_{i\uparrow} n_{j\downarrow} + (U' - J) \sum_{i < j, \sigma} n_{i\sigma} n_{j\sigma} - J \sum_{i \neq j} c_{i\uparrow}^\dagger c_{i\downarrow} c_{j\downarrow}^\dagger c_{j\uparrow} + J \sum_{i \neq j} c_{i\uparrow}^\dagger c_{i\downarrow}^\dagger c_{j\downarrow} c_{j\uparrow}$$

t_{2g} model



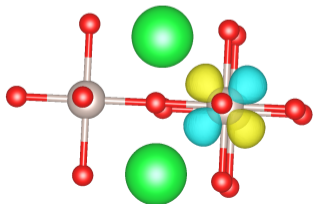
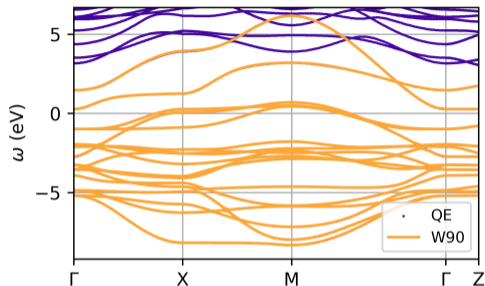
pros:

- no DC
- nominal occupations
- less work for impurity solver

cons:

- smaller U , more frequency-dependent
- larger spread Ω , oxygen tails \rightarrow less localized
- no information on e_g states...

dp model



pros:

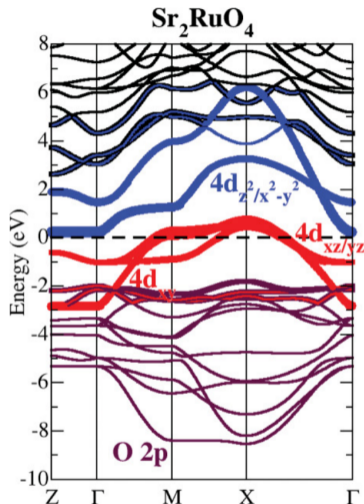
- more localized, DMFT more valid
- larger U and more atomic-like, less frequency-dependent
- renormalizes all states

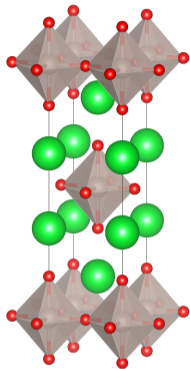
cons:

- DC, in principle U_{dp}, U_p
- fractional occupations
- heavy for impurity solver

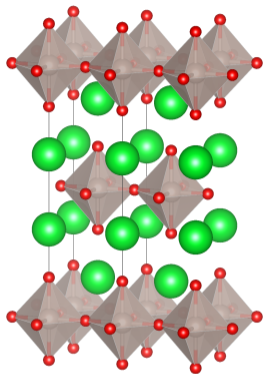
How to determine Coulomb interaction

- V of the order of 11 eV for t_{2g} ,
i.e. \gg bandwidth ≈ 3.4 eV
- effective Coulomb interaction screened by
surrounding electrons
- screened interaction $U(\mathbf{r}, \mathbf{r}')$ in practice:
 - cRPA: screening channels, frequency
dependence, Hund J
 - cLDA: only full d shell, static, no Hund J
- $d - dp$: $F^0 = 3.23$ eV, $\bar{U}_{mm} = 4.1$ eV,
 $t_{2g} - t_{2g}$: $\mathcal{U} = 2.56$ eV



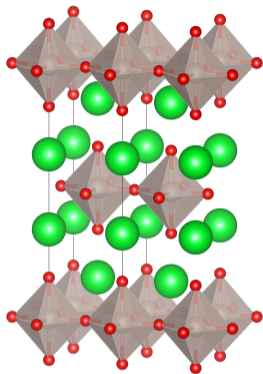


$$\Sigma = \left(\boxed{\Sigma_{\text{imp}}} \right)$$



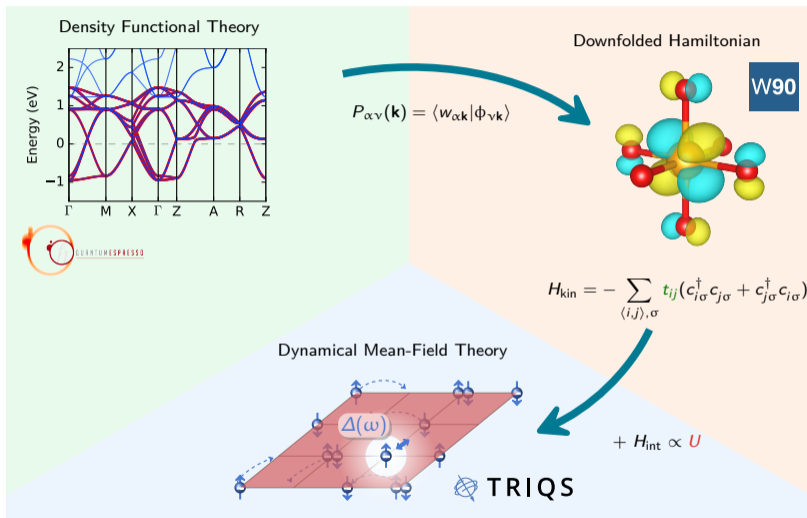
$$\Sigma = \begin{pmatrix} \Sigma_{\text{imp}}^1 & & & \\ & \Sigma_{\text{imp}}^2 & & \\ & & \Sigma_{\text{imp}}^3 & \\ & & & \Sigma_{\text{imp}}^4 \end{pmatrix}$$

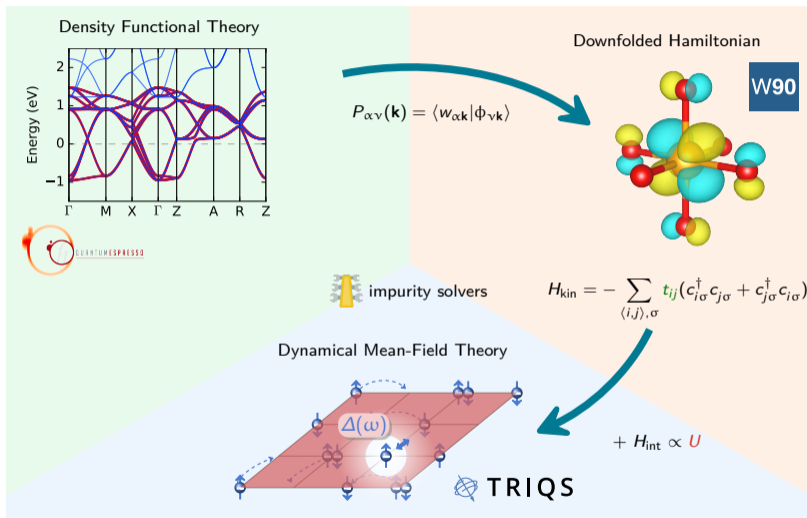
- self-energy approximated as block-diagonal in orbital basis

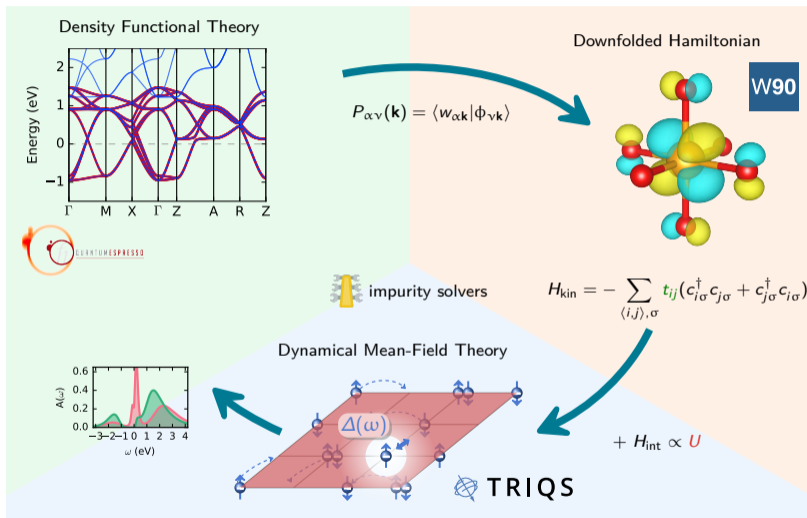


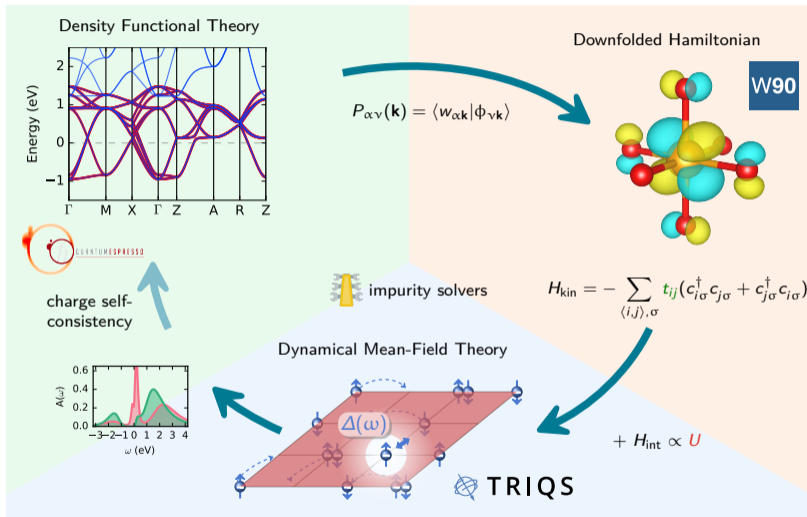
$$\Sigma = \left(\begin{array}{cccc} \Sigma_{\text{imp}}^1 & & & \\ & \square & & \\ & & \square & \\ & & & \square \end{array} \right)$$

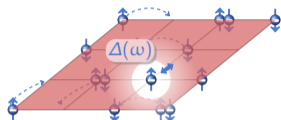
- self-energy approximated as block-diagonal in orbital basis
- map self-energy to symmetry-equivalent sites
- use spin channel for AFM solutions











$$G_{\sigma}^{\text{imp}}(\tau) = \langle T c_{\sigma}(\tau) c_{\sigma}^{\dagger}(0) \rangle_{\mathcal{G}_0}$$



approximate solvers:

- Hartree(-Fock)
- Hubbard-I
- Iterated perturbation theory (IPT)
- Slave boson technique
- ...

numerically exact solvers:

- Quantum Monte Carlo (QMC)
- exact diagonalization (ED)
- numerical renormalization group (NRG)
- density matrix renormalization group (DMRG)
- tensor-network based approaches (MPS/TTN)

Method	Physical quantity	Constraining field
Baym-Kadanoff	$G_{\alpha\beta}(\mathbf{k}, i\omega)$	$\Sigma_{\text{int},\alpha\beta}(\mathbf{k}, i\omega)$
DMFT (BL)	$G_{\text{loc},\alpha\beta}(i\omega)$	$\mathcal{M}_{\text{int},\alpha\beta}(i\omega)$
DMFT (AL)	$G_{\text{loc},\alpha\beta}(i\omega)$	$\Delta_{\alpha\beta}(i\omega)$
LDA+DMFT (BL)	$\rho(r), G_{\text{loc},ab}(i\omega)$	$V_{\text{int}}(r), \mathcal{M}_{\text{int},ab}(i\omega)$
LDA+DMFT (AL)	$\rho(r), G_{\text{loc},ab}(i\omega)$	$V_{\text{int}}(r), \Delta_{ab}(i\omega)$
LDA+ U	$\rho(r), n_{ab}$	$V_{\text{int}}(r), \lambda_{ab}$
LDA	$\rho(r)$	$V_{\text{int}}(r)$

interacting charge density

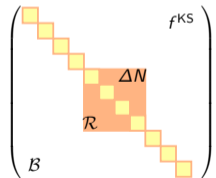
$$\rho(\mathbf{r}) = \frac{1}{\beta} \sum_{n,\mathbf{k}} \langle \mathbf{r} | \hat{G}(\mathbf{k}, i\omega_n) | \mathbf{r} \rangle \equiv \rho^{\text{KS}}(\mathbf{r}) + \Delta\rho(\mathbf{r})$$

KS charge density:

$$\rho^{\text{KS}}(\mathbf{r}) = \sum_{\mathbf{k}} \sum_{n=1}^{N_{\mathcal{B}}} f_{\nu\mathbf{k}}^{\text{KS}} \langle \mathbf{r} | \psi_{n\mathbf{k}} \rangle \langle \psi_{n\mathbf{k}} | \mathbf{r} \rangle$$

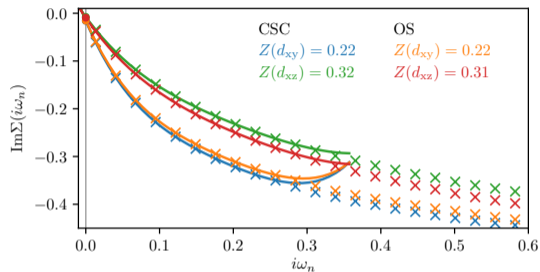
→ compute $\Delta\rho(\mathbf{r})$, feed it back to DFT, compute updated KS charge density $\rho^{\text{KS}}(\mathbf{r})$

$$\begin{aligned} \Delta\rho(\mathbf{r}) &= \frac{1}{\beta} \sum_{n,\mathbf{k}} \langle \mathbf{r} | \hat{G}(\mathbf{k}, i\omega_n) - \hat{G}^{\text{KS}}(\mathbf{k}, i\omega_n) | \mathbf{r} \rangle \\ &\equiv \sum_{\mathbf{k}} \langle \mathbf{r} | \Delta\hat{N}(\mathbf{k}) | \mathbf{r} \rangle \end{aligned}$$

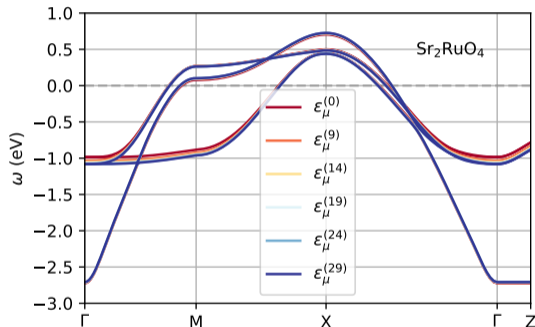
$$\hat{N}(\mathbf{k}) = \begin{pmatrix} \text{matrix} & f^{\text{KS}} \\ \mathcal{R} & \Delta N \\ \mathcal{B} & \end{pmatrix}$$


F. Lechermann *et al.*, Phys. Rev. B 74, 125120 (2006)

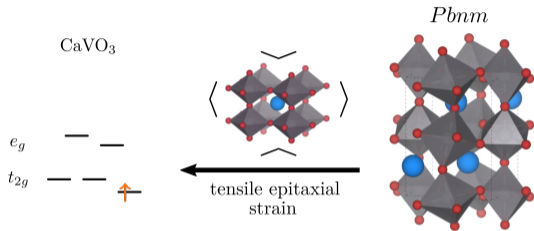
M. Schüler *et al.*, J. Phys. Condens. Matter 30, 475901 (2018)



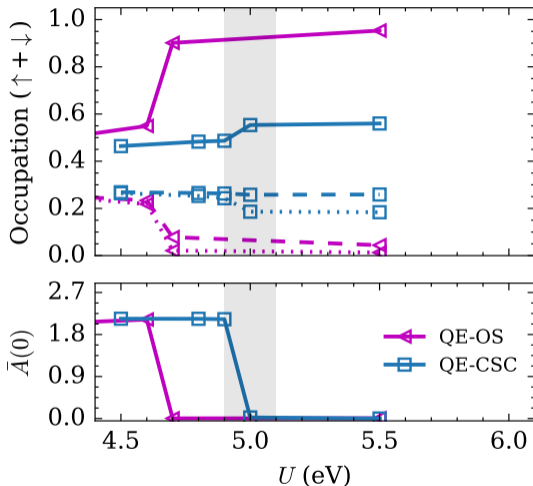
- CT-HYB solver, $\beta = 232 \text{ eV}^{-1}$
- minimal effect of charge self-consistency



Orbital polarization in CaVO_3 (tensile strain)



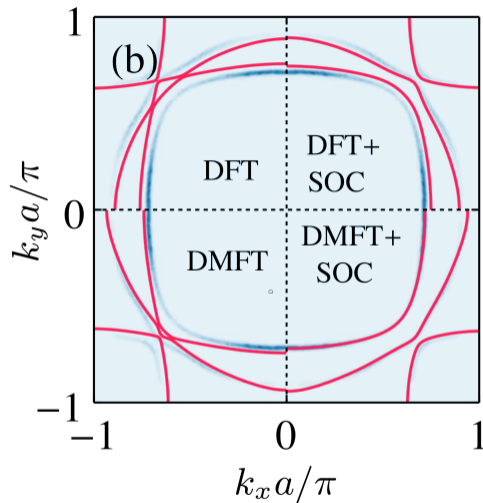
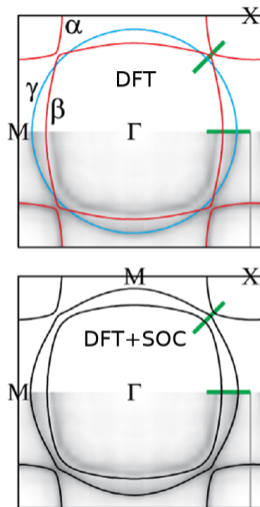
- CT-HYB solver, $\beta = 40 \text{ eV}^{-1}$
- charge self-consistency strongly reduces the orbital polarization found in one-shot calculations



What we can compute:

- spectral properties
- optical and thermal conductivity
- Hall and Seebeck coefficient
- two-particle correlation function (susceptibilities)
- ...
- electronic Raman spectroscopy
- x-ray photoemission and absorption spectroscopy
- resonant inelastic x-ray scattering
- phonon spectra

Back to the experiment



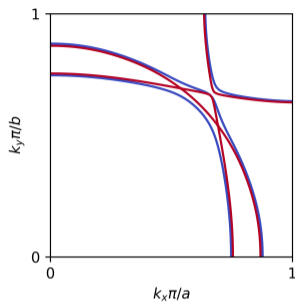
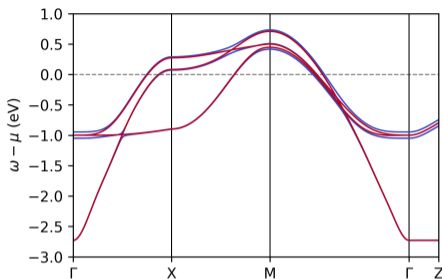
M. W. Haverkort *et al.*, Phys. Rev. Lett. 101, 026406 (2008)

A. Tamai *et al.*, Phys. Rev. X 9, 021048 (2019)

X. Cao *et al.*, Phys. Rev. B 104, 115119 (2021)

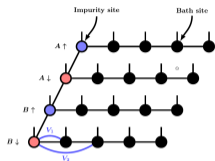
spin-orbit coupling λ

$$c_{ij} = \begin{pmatrix} \epsilon_{xy} & 0 & 0 & 0 & \frac{\lambda_{xy}}{2} & \frac{i\lambda_{xy}}{2} \\ 0 & \epsilon_{yz} & -\frac{i\lambda_x}{2} & -\frac{\lambda_{xy}}{2} & 0 & 0 \\ 0 & \frac{i\lambda_x}{2} & \epsilon_{xz} & -\frac{i\lambda_{xy}}{2} & 0 & 0 \\ 0 & -\frac{\lambda_{xy}}{2} & \frac{i\lambda_{xy}}{2} & \epsilon_{xy} & 0 & 0 \\ \frac{\lambda_{xy}}{2} & 0 & 0 & 0 & \epsilon_{yz} & \frac{i\lambda_x}{2} \\ -\frac{i\lambda_{xy}}{2} & 0 & 0 & 0 & -\frac{i\lambda_x}{2} & \epsilon_{xz} \end{pmatrix}$$



$$\hat{H}_\lambda^{\text{SOC}} = \frac{\lambda}{2} \sum_{ij} \sum_{\sigma\sigma'} c_{i\sigma}^\dagger (\mathbf{l}_{ij} \cdot \boldsymbol{\sigma}_{\sigma\sigma'}) c_{j\sigma'}$$

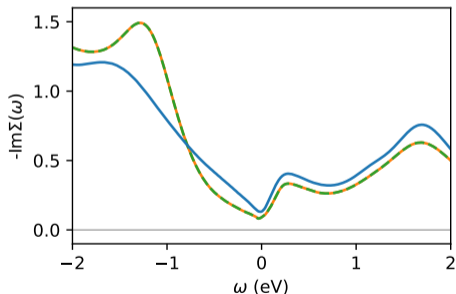
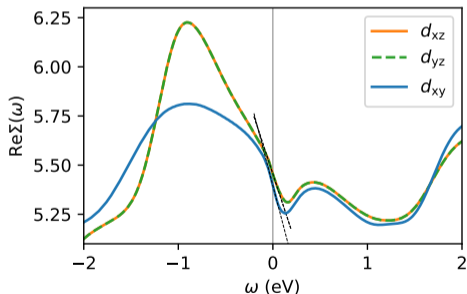
- correlation-induced enhancement of crystal-field splitting
- correlation-induced enhancement of effective spin-orbit coupling



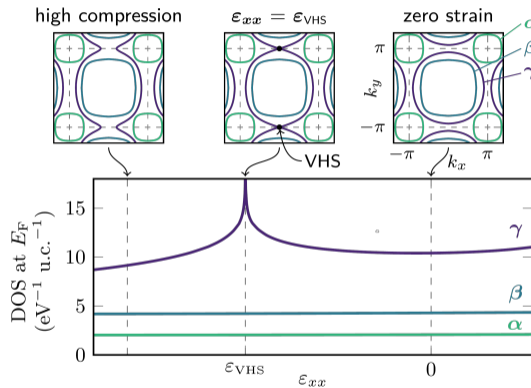
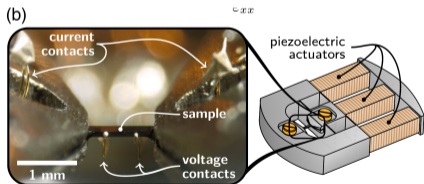
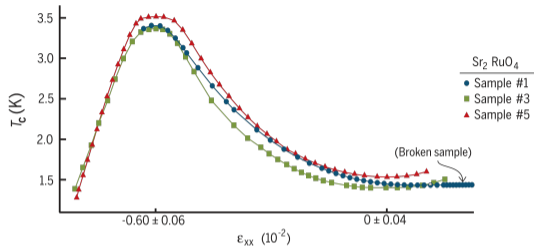
self-energy from ForkTPS:

$$\Sigma(\omega) = \Sigma'(\omega) + i\Sigma''(\omega)$$

$$A(\mathbf{k}, \omega) = \frac{1}{\pi} \frac{\Sigma''(\omega)}{(\omega - \epsilon_{\mathbf{k}} - \Sigma'(\omega))^2 + \Sigma''(\omega)^2}$$



Sr₂RuO₄ under uniaxial pressure

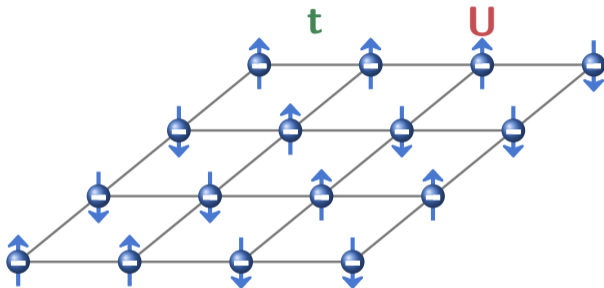


A. Steppke *et al.*, Science 355, eaaf9398 (2017)

M. E. Barber *et al.*, Phys. Rev. Lett. 120, 076602 (2018)

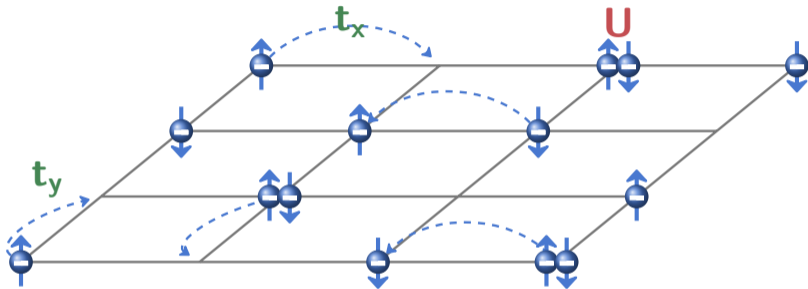
Uniaxial strain experiments

$$H = - \sum_{\langle ij \rangle \sigma} t_{ij} c_{i\sigma}^\dagger c_{j\sigma} + U \sum_i n_{i\uparrow} n_{i\downarrow}$$



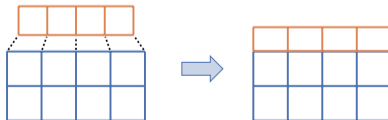
Uniaxial strain experiments

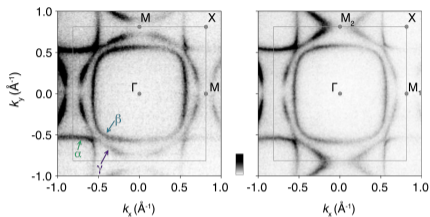
$$H = - \sum_{\langle ij \rangle \sigma} t_{ij} c_{i\sigma}^\dagger c_{j\sigma} + U \sum_i n_{i\uparrow} n_{i\downarrow}$$



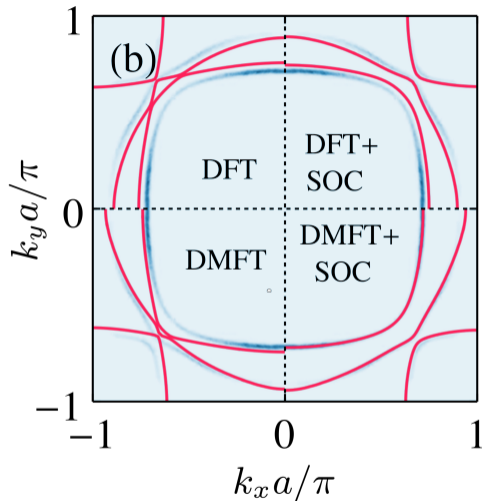
Film:

Substrate:





- Lifshitz transition with uniaxial strain
- novel FTPS impurity solver, including spin-orbit coupling
- critical strain $\epsilon_{xx} \approx -0.4$ consistent with experiment



V. Sunko *et al.*, npj Quantum Mater. 4, 46 (2019)

M. E. Barber *et al.*, Phys. Rev. B 100, 245139 (2019)

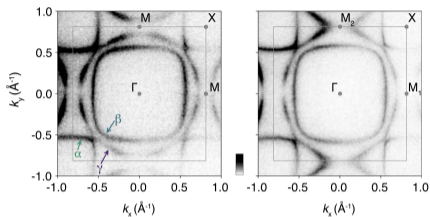
sbeck@flatironinstitute.org

D. Bauernfeind *et al.*, Phys. Rev. X 7, 031013 (2017)

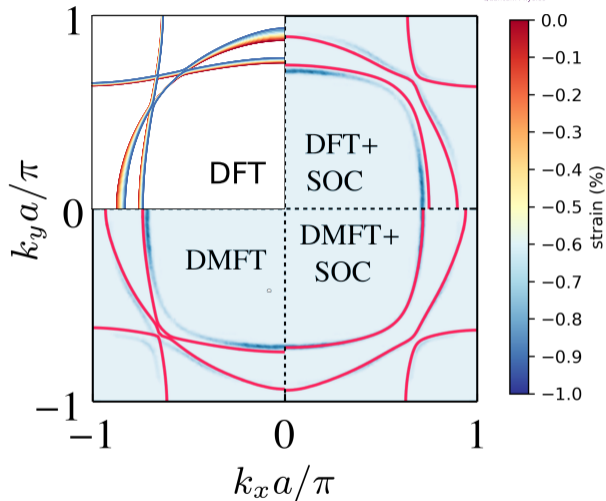
X. Cao *et al.*, Phys. Rev. B 104, 115119 (2021)

TRIQS summer school 2023

Pressure-driven Lifshitz transition in Sr_2RuO_4



- Lifshitz transition with uniaxial strain
- novel FTPS impurity solver, including spin-orbit coupling
- critical strain $\epsilon_{xx} \approx -0.4$ consistent with experiment



V. Sunko *et al.*, npj Quantum Mater. 4, 46 (2019)

M. E. Barber *et al.*, Phys. Rev. B 100, 245139 (2019)

sbeck@flatironinstitute.org

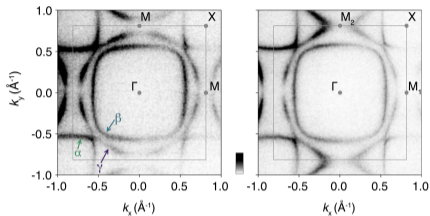
D. Bauernfeind *et al.*, Phys. Rev. X 7, 031013 (2017)

X. Cao *et al.*, Phys. Rev. B 104, 115119 (2021)

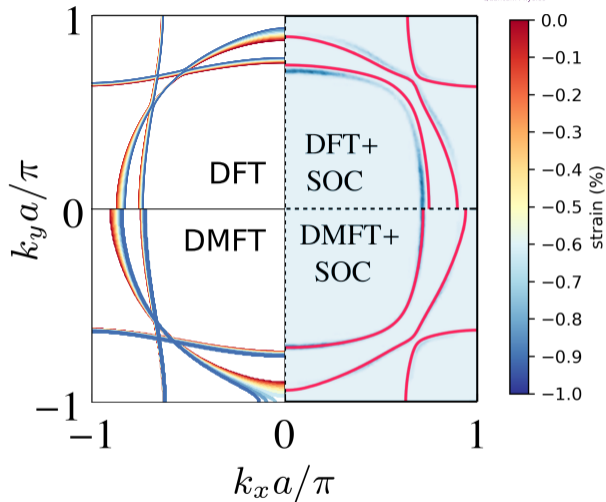
TRIQS summer school 2023

40

Pressure-driven Lifshitz transition in Sr_2RuO_4



- Lifshitz transition with uniaxial strain
- novel FTPS impurity solver, including spin-orbit coupling
- critical strain $\epsilon_{xx} \approx -0.4$ consistent with experiment



V. Sunko *et al.*, npj Quantum Mater. 4, 46 (2019)

M. E. Barber *et al.*, Phys. Rev. B 100, 245139 (2019)

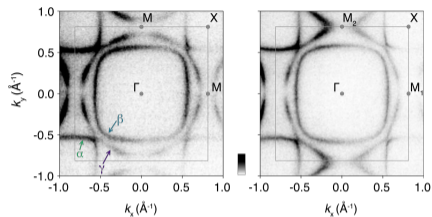
sbeck@flatironinstitute.org

D. Bauernfeind *et al.*, Phys. Rev. X 7, 031013 (2017)

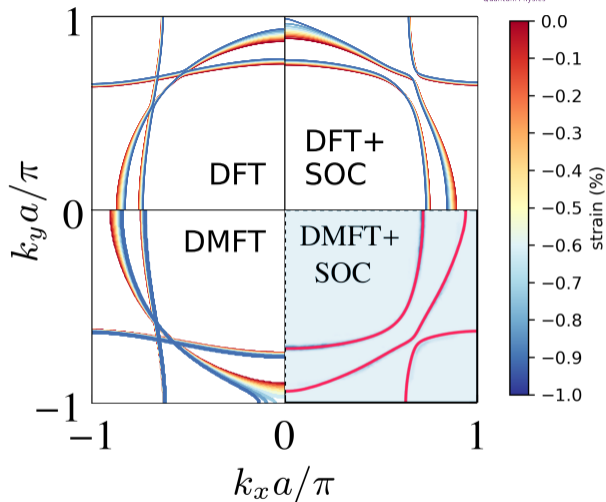
X. Cao *et al.*, Phys. Rev. B 104, 115119 (2021)

TRIQS summer school 2023

Pressure-driven Lifshitz transition in Sr_2RuO_4



- Lifshitz transition with uniaxial strain
- novel FTPS impurity solver, including spin-orbit coupling
- critical strain $\epsilon_{xx} \approx -0.4$ consistent with experiment



V. Sunko *et al.*, npj Quantum Mater. 4, 46 (2019)

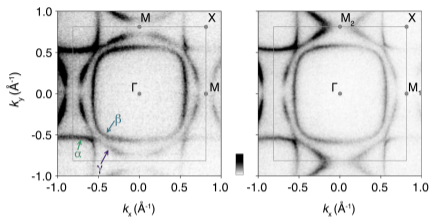
M. E. Barber *et al.*, Phys. Rev. B 100, 245139 (2019)

sbeck@flatironinstitute.org

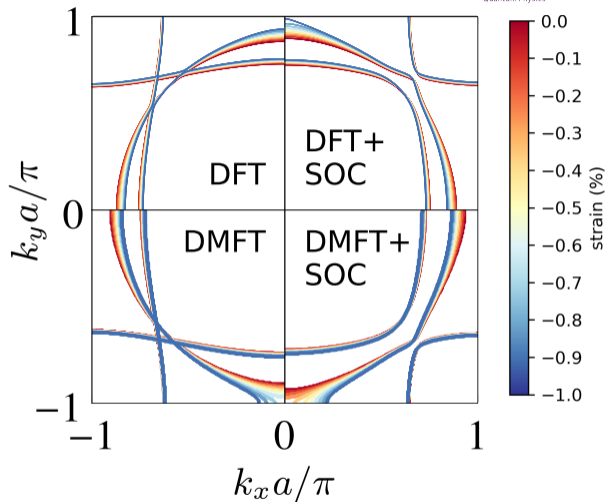
D. Bauernfeind *et al.*, Phys. Rev. X 7, 031013 (2017)

X. Cao *et al.*, Phys. Rev. B 104, 115119 (2021)

TRIQS summer school 2023



- Lifshitz transition with uniaxial strain
- novel FTPS impurity solver, including spin-orbit coupling
- critical strain $\epsilon_{xx} \approx -0.4$ consistent with experiment



V. Sunko *et al.*, npj Quantum Mater. 4, 46 (2019)

M. E. Barber *et al.*, Phys. Rev. B 100, 245139 (2019)

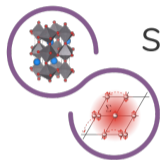
sbeck@flatironinstitute.org

D. Bauernfeind *et al.*, Phys. Rev. X 7, 031013 (2017)

X. Cao *et al.*, Phys. Rev. B 104, 115119 (2021)

TRIQS summer school 2023

40



solid_dmft

A versatile python wrapper to perform DFT + DMFT calculations utilizing the TRIQS software library.



M. Merkel
(ETHZ)



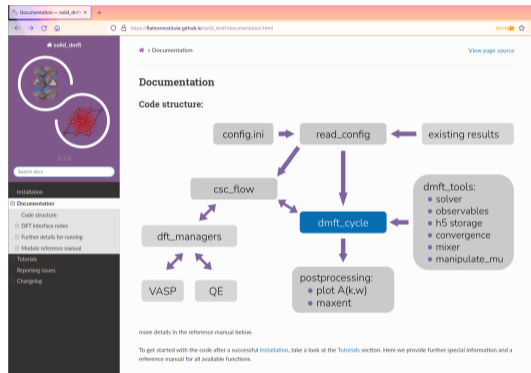
A. Carta
(ETHZ)



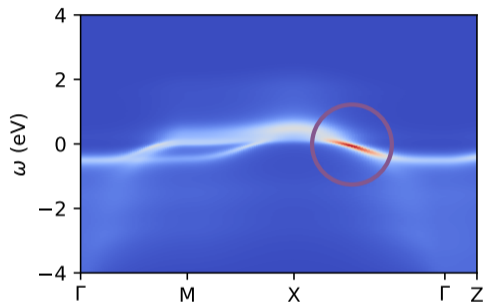
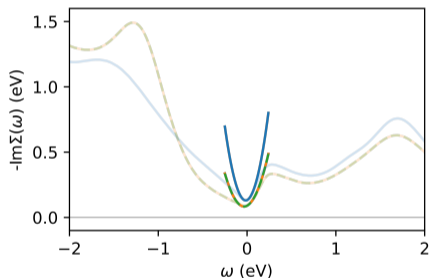
S. Beck



A. Hampel



$$\Sigma(\omega, T) \propto -\frac{i}{Z\alpha} [\omega^2 + (\pi k_B T)^2]$$

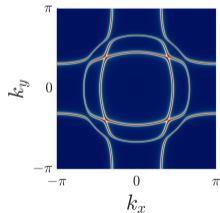
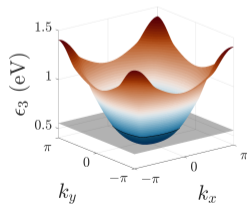
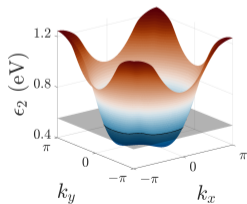
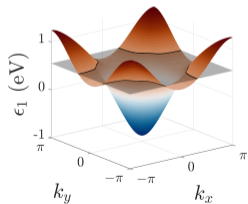


- scattering rate finite but possibly extremely small
- frequency dependence requires adaptivity for momentum integration

Automatic, high-order, adaptive Brillouin zone integration

Task: compute local single-particle Green's function (i.e. DOS)

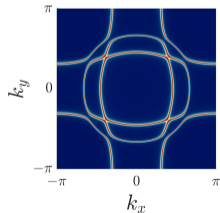
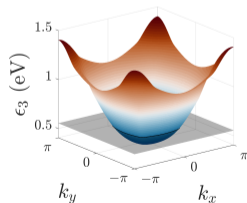
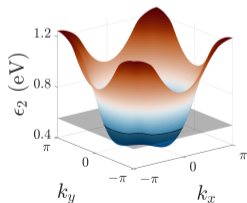
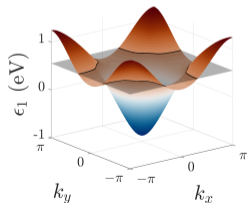
$$G(\omega) = \int_{\text{BZ}} d^3\mathbf{k} \text{Tr} \left[(\omega - H(\mathbf{k}) - \Sigma(\mathbf{k}, \omega))^{-1} \right]$$



Task: compute local single-particle Green's function (i.e. DOS)

$$G(\omega) = \int_{\text{BZ}} d^3\mathbf{k} \text{Tr} \left[(\omega - H(\mathbf{k}) - \Sigma(\mathbf{k}, \omega))^{-1} \right]$$

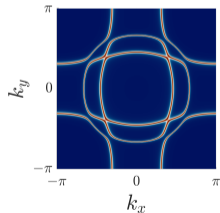
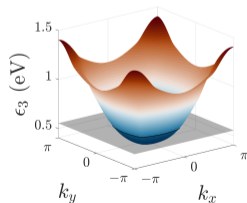
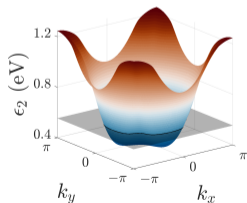
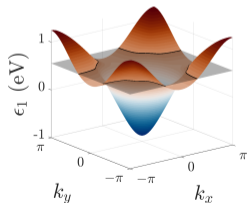
- **Applications:** self-consistency loops in DMFT and post-processing



Task: compute local single-particle Green's function (i.e. DOS)

$$G(\omega) = \int_{\text{BZ}} d^3\mathbf{k} \text{Tr} \left[(\omega - H(\mathbf{k}) - \Sigma(\mathbf{k}, \omega))^{-1} \right]$$

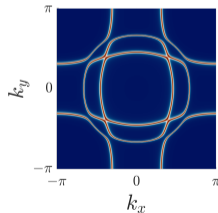
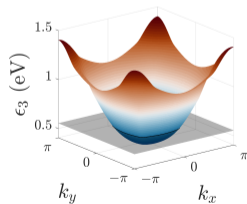
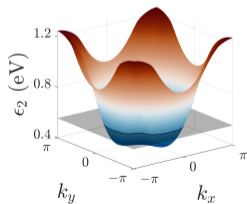
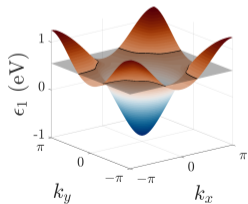
- **Applications:** self-consistency loops in DMFT and post-processing
- **Setting:** $H(\mathbf{k})$ obtained from a Wannier Hamiltonian $H(\mathbf{R})$, $\Sigma(\mathbf{k}, \omega) = i\eta$

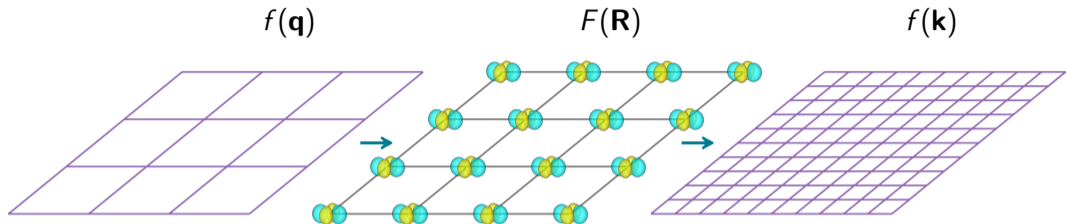


Task: compute local single-particle Green's function (i.e. DOS)

$$G(\omega) = \int_{\text{BZ}} d^3\mathbf{k} \text{Tr} \left[(\omega - H(\mathbf{k}) - \Sigma(\mathbf{k}, \omega))^{-1} \right]$$

- **Applications:** self-consistency loops in DMFT and post-processing
- **Setting:** $H(\mathbf{k})$ obtained from a Wannier Hamiltonian $H(\mathbf{R})$, $\Sigma(\mathbf{k}, \omega) = i\eta$
- **Goal:** fully automatic, high-order and adaptive algorithm





$$\mathcal{O}_{nm}(\mathbf{q}) = \langle u_{n\mathbf{q}} | \hat{\mathcal{O}}(\mathbf{q}) | u_{m\mathbf{q}} \rangle$$

$$\mathcal{O}_{nm}^{(W)}(\mathbf{R}) = \frac{1}{N_0} \sum_{\mathbf{q}} e^{-i\mathbf{q}\cdot\mathbf{R}} \mathcal{O}_{nm}^{(W)}(\mathbf{q})$$

$$\mathcal{O}_{nm}^{(W)}(\mathbf{k}) = \sum_{\mathbf{R}} e^{i\mathbf{k}\cdot\mathbf{R}} \mathcal{O}_{nm}^{(W)}(\mathbf{R})$$

- periodic trapezoidal rule (PTR):

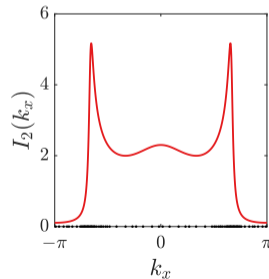
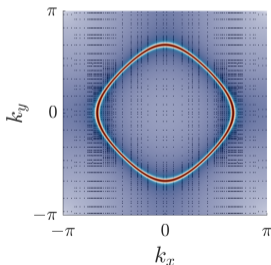
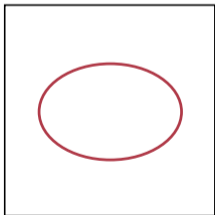
$$\mathcal{O}(\eta^{-3})$$

- iterated adaptive integration (IAI)¹:

$$\mathcal{O}(\log^3(\eta^{-1}))$$

$$\int \int dk_x dk_y f(k_x, k_y) = \int dk_x I_2(k_x),$$

$$I_2(k_x) = \int dk_y f(k_x, k_y)$$

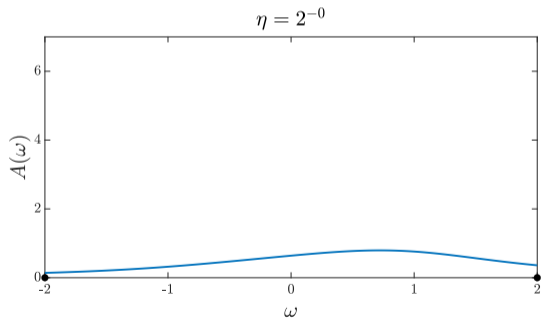
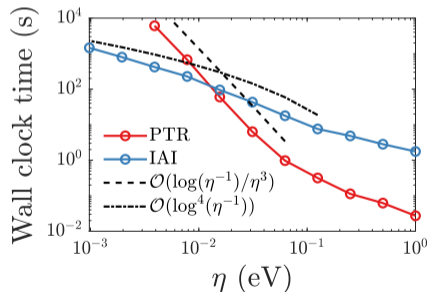
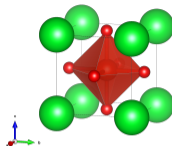


¹J. Kaye, SB, A. Barnett, L. Van Muñoz, and O. Parcollet, arxiv:2211.12959 (2022)

Example: density of states

DOS of SrVO₃, three t_{2g} orbitals:

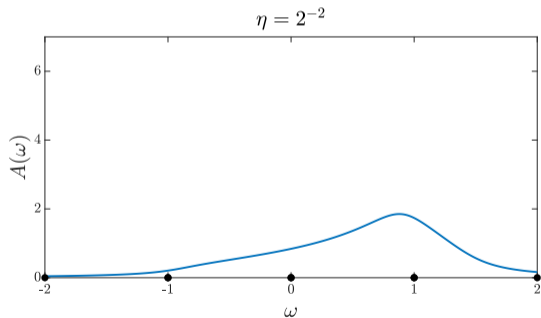
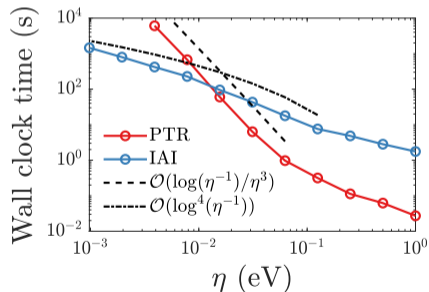
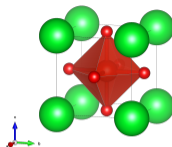
$$A(\omega) = -\frac{1}{\pi} \text{Im}G(\omega) = -\frac{1}{\pi} \text{Im} \int_{\text{BZ}} d^3\mathbf{k} \text{Tr} \left[(\omega - H(\mathbf{k}) - i\eta)^{-1} \right]$$



Example: density of states

DOS of SrVO₃, three t_{2g} orbitals:

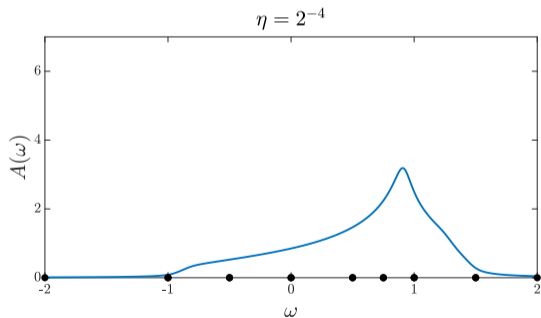
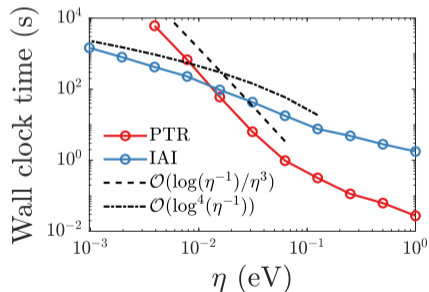
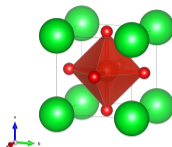
$$A(\omega) = -\frac{1}{\pi} \text{Im}G(\omega) = -\frac{1}{\pi} \text{Im} \int_{\text{BZ}} d^3\mathbf{k} \text{Tr} \left[(\omega - H(\mathbf{k}) - i\eta)^{-1} \right]$$



Example: density of states

DOS of SrVO₃, three t_{2g} orbitals:

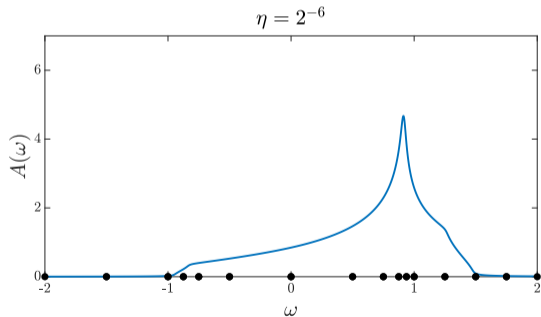
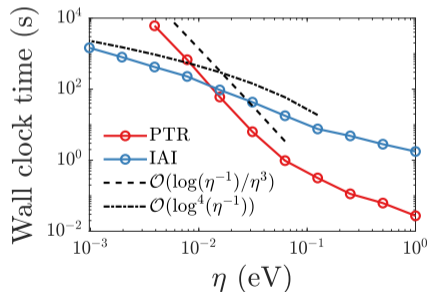
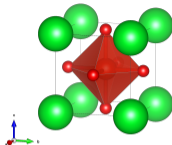
$$A(\omega) = -\frac{1}{\pi} \text{Im}G(\omega) = -\frac{1}{\pi} \text{Im} \int_{\text{BZ}} d^3\mathbf{k} \text{Tr} \left[(\omega - H(\mathbf{k}) - i\eta)^{-1} \right]$$



Example: density of states

DOS of SrVO₃, three t_{2g} orbitals:

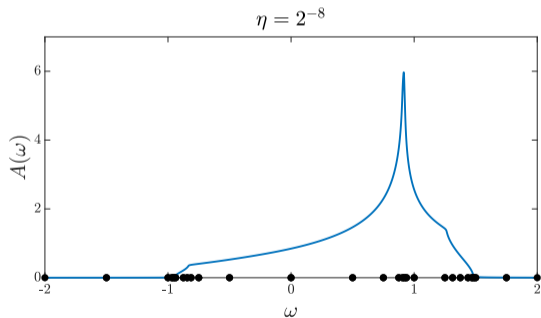
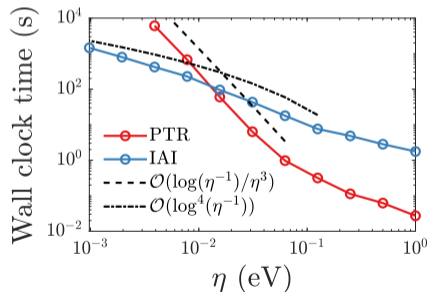
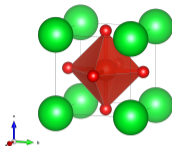
$$A(\omega) = -\frac{1}{\pi} \text{Im}G(\omega) = -\frac{1}{\pi} \text{Im} \int_{\text{BZ}} d^3\mathbf{k} \text{Tr} \left[(\omega - H(\mathbf{k}) - i\eta)^{-1} \right]$$



Example: density of states

DOS of SrVO₃, three t_{2g} orbitals:

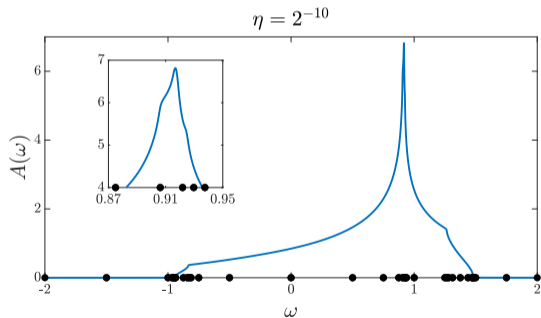
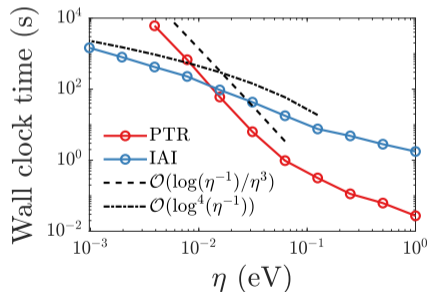
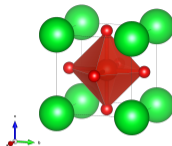
$$A(\omega) = -\frac{1}{\pi} \text{Im}G(\omega) = -\frac{1}{\pi} \text{Im} \int_{\text{BZ}} d^3\mathbf{k} \text{Tr} \left[(\omega - H(\mathbf{k}) - i\eta)^{-1} \right]$$

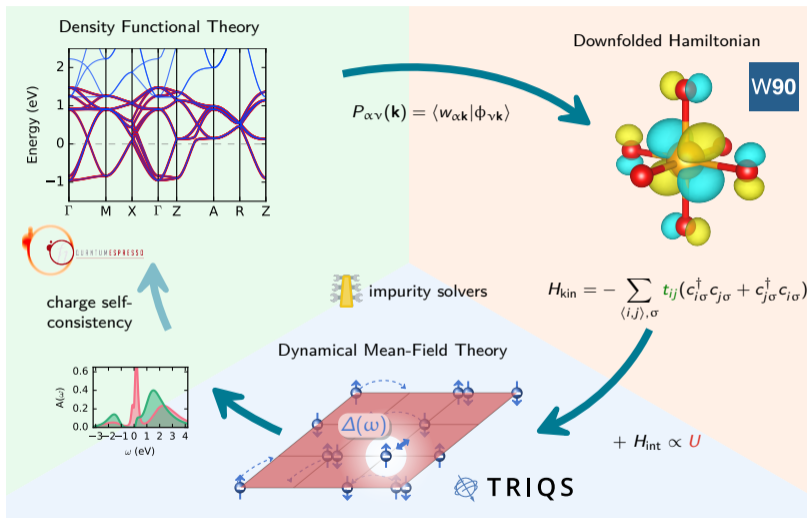


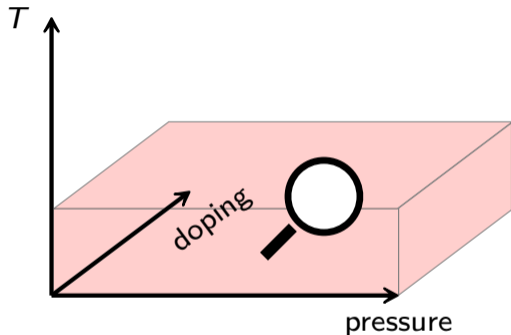
Example: density of states

DOS of SrVO₃, three t_{2g} orbitals:

$$A(\omega) = -\frac{1}{\pi} \text{Im}G(\omega) = -\frac{1}{\pi} \text{Im} \int_{\text{BZ}} d^3\mathbf{k} \text{Tr} \left[(\omega - H(\mathbf{k}) - i\eta)^{-1} \right]$$







- double counting
- more orbitals, more complex systems
- screening
- (real-frequency) impurity solvers and analytic continuation
- superconductivity
- out of equilibrium
- low- T , exotic states